Journal of the Association for Research in Otolaryngology
https://doi.org/10.1007/s10162-026-01069-5

JARO

ORIGINAL ARTICLE

Gain-Delay Decoupling in Human Stimulus Frequency Otoacoustic Emissions Reveals Constraints on Cochlear Nonlinear Amplification

Yoshita Sharma[1] · Arturo Moleti[1] · Renata Sisto[2] · Teresa Botti[2] · Hansapani Rodrigo[3] · Srikanta K. Mishra[4]

Received: 10 March 2026 / Accepted: 6 August 2026

Abstract

Purpose The nonlinear cochlear amplifier, driven by outer hair cells, underlies the remarkable sensitivity and frequency selectivity of the mammalian auditory system. Stimulus frequency otoacoustic emissions (SFOAEs) provide a noninvasive window into these active cochlear processes, yet the relationship between emission gain and delay across stimulus levels remains incompletely understood. This study examined the level dependence of SFOAEs in normal-hearing human listeners to characterize cochlear nonlinear response properties. We tested how emission gain and delay vary with stimulus level and estimated the frequency of the apical–basal transition associated with the breakdown of the approximate local scaling symmetry.

Methods SFOAEs were recorded from a cohort of normal-hearing participants ($n = 20$; females = 13) across a range of stimulus levels. A time-frequency filtering approach was applied to isolate single-reflection components and improve signal-to-noise ratio, yielding stable and unbiased estimates of emission level and phase-gradient delay. The relationships between stimulus level, gain, and delay were analyzed and normalized using a general relation derived from the fundamental physical properties of linear two-dimensional cochlear model.

Results The results confirm the nonlinear dependence of SFOAE level and delay on stimulus level. However, when the variations in gain and delay were compared to the predictions of a linear and a nonlinear 2D cochlear model, the discrepancy with the linear model predictions was evident. Measurements also revealed no stimulus-level dependence of the apical–basal transition frequency, consistent with a fixed apical cochlear region associated with the breakdown of the approximate scaling symmetry.

Conclusion The relative decoupling between gain and delay indicates that changes in cochlear amplification do not produce proportionate changes in emission timing, revealing constraints on the relationship between amplification and phase behavior in human cochlear responses. These findings indicate that SFOAE delay may remain informative about cochlear tuning, but nonlinear cochlear models could be constrained by the observed decoupling between gain and delay.

Keywords Cochlear gain and delay · Cochlear nonlinearity · Cochlear tuning · Otoacoustic emissions · SFOAEs

Introduction

Stimulus frequency otoacoustic emissions (SFOAEs) are assumed to be generated in the cochlea by coherent reflection of the forward traveling wave (TW) generated by the stimulus tone, due to cochlear roughness [1, 2]. Independent of the nature of roughness, the mechanism selects a discrete set of wavenumbers and frequencies that dominate the SFOAEs, which appear as discrete spots of given delay and frequency in the time-frequency representation of the response [3, 4]. The main spots belong to a curved band centered on the hyperbolic-like curve that represents the average delay of single-reflection

✉ Srikanta K. Mishra
srikanta.mishra@austin.utexas.edu

1 Physics Department, University of Roma Tor Vergata, Via della Ricerca Scientifica, 1, 00134 Rome, Italy

2 DIMEILA, INAIL, Via di Fontana Candida, 1, 00078 Monte Porzio Catone, RM, Italy

3 School of Mathematical and Statistical Sciences, The University of Texas Rio Grande Valley, Edinburg, TX 78539, USA

4 Speech, Language, & Hearing Sciences, University of Texas at Austin, Austin, TX 78712-0114, USA

Published online: 01 September 2026

components (dashed line in Fig. 1). Within the single-reflection band, a further temporal structure may be noted, with spots of longer/shorter delay associated with reflections from more apical–basal regions, within the spatial region of the response peak. The relative weight of basal sources increases with stimulus level; therefore, the SFOAE delay slowly decreases with increasing stimulus level [3].

The SFOAE phase gradient delay has been widely considered an objective indicator of cochlear tuning in humans [3–11]. Indeed, based on general filter theory, the roundtrip delay of the TW from the base to the generation region should be related to the bandwidth of the BM frequency response at that location. This relation would be straightforward in the case of a simple passive resonant system, or of a nonlinear second-order filter in the long wave approximation [9]. Supporting this interpretation, BM delay and tuning have been shown to vary similarly with stimulus level, and the ratio between BM delay and the delay of coherent reflection OAEs, including transient-evoked and SF-OAEs, remains approximately constant over a wide range of stimulus levels [12].

On the other hand, classical experiments on animal models, reviewed in Robles and Ruggero [13], and more recent optical coherence tomography experiments (e.g., [14, 15]) show that the pronounced level dependence of BM gain is not accompanied by similarly large changes in BM phase slope or tuning. As discussed in Sisto et al. [16] for a few models, fully nonlinear cochlear models with instantaneous nonlinearity also tend to predict a response in which phase-gradient delay is significantly decoupled from gain, with respect to the corresponding linear models. This gain-delay decoupling does not invalidate the relationship between delay and tuning, because delay and tuning may still vary. Rather, it will be shown that the quantitative relation between SFOAE delay and gain changes must be evaluated and interpreted within a model that captures nonlinear cochlear mechanics.

Recent cochlear modeling studies (i.e., [17, 18]) have demonstrated that, also in the linear approximation, the cochlear response is much different from that of a second-order filter. Indeed, the spatial shape of the cochlear response to tones is determined by the interplay of two mechanisms: the 2D hydrodynamic boost known as pressure focusing [19, 20] and the increasing viscous losses. Both phenomena increase proportionally to the local wavenumber, approaching the best place (BP), which we define here as the place where the response to a tone of given frequency and level peaks, determined by a balance between viscous losses and anti-damping power input from the OHC electromotility. Considering the nonlinear nature of the OHC electromotility, with increasing stimulus level, this power balance is obtained at BPs that are increasingly basally shifted with respect to the characteristic place (CP), which we define here as the place where the imaginary part of the local admittance has a minimum. If one uses a rough parametrization of nonlinearity and computes the response of a set of linear systems of different OHC gain to schematize the dependence on stimulus level, the resulting response peak level, width, and position are not those of a resonant system, but the result of the interplay of focusing, viscosity, and anti-damping level. While phase-gradient delay depends on the slope of the phase function in the peak region, tuning depends on the width of the peak, i.e., also on the position/frequency if the abrupt drop is caused by viscous losses. Therefore, even in linear 2D models, different models could also predict, in principle, slightly different relations between mechanical BM tuning and delay, as we will discuss later. The experimental covariance between delay and tuning observed in animals [12] and the relation between BM and OAE delays confirmed also for humans by comparing ABR and OAE data [21, 22] suggest that this is not invalidating the SFOAE-based estimates of tuning, but the sharper tuning of humans could further complicate the issue.

Psychophysical tuning curves (PTCs) are behavioral estimates of cochlear frequency selectivity, reflecting the combined effects of cochlear filtering, gain, and compression, although they may also be influenced by more central auditory processes [7, 23]. Therefore, changes in PTC bandwidth with level are often interpreted as indirect evidence of level-dependent changes in cochlear gain and mechanics,

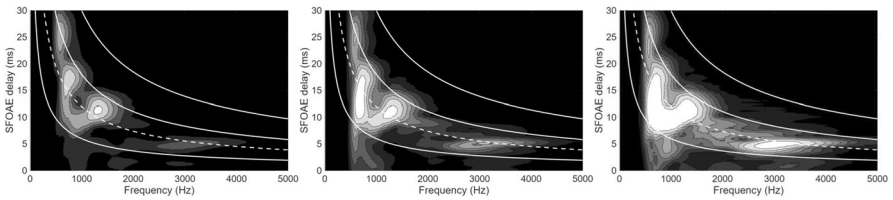

Fig. 1 Time-frequency representation of the SFOAEs of one subject for three stimulus levels (20, 30, and 40 dB FPL, from left to right). Intensity is represented by brightness, using the same absolute scale for all plots. Single-reflection SFOAEs are distributed within the region between the two lower solid lines, with the sub-regions above (long latency, LL) and below the dashed line (short latency, SL) associated, respectively, with more apical and more basal sources, within the response peak region

which can be compared with OAE-based measures of delay and tuning. The extent to which PTCs depend on stimulus level or measurement procedure has been debated, but the literature suggests a nuanced picture. Early work by Weber [24] demonstrated that behavioral tuning curves derived from forward masking are procedure independent: fixed-masker and fixed-signal paradigms yield the same growth-of-masking functions, indicating that the tuning curve is not influenced by whether masker or signal level is treated as the dependent variable. Similarly, Ewert and Dau [25] reported that modulation-based PTCs are largely independent of absolute stimulus level within the tested range, provided the signal is maintained just above threshold and the masker is set adaptively at the masking point. In contrast, clear level dependence emerges when masker levels increase substantially. Nelson et al. [26] showed that forward-masked PTCs broaden as probe level increases, primarily because higher probe levels require higher masker levels at the tip (Lm tip); once Lm tip exceeds ~ 60 dB SPL, low-frequency slopes flatten and Q_{10} dB values decrease markedly, whereas curves remain relatively invariant below this level. Extending this interpretation, Lopez-Poveda et al. [27] demonstrated that tuning-curve bandwidth broadens at lower effective cochlear gain and that activation of the medial olivocochlear reflex further enhances this level dependence by reducing cochlear gain (notably at 500 Hz), thereby broadening the PTC. Taken together, these findings indicate that while the measurement procedure itself does not bias tuning-curve shape, the effective stimulus level at the cochlea, particularly as reflected in masker level at the tip and cochlear gain, plays a critical role in determining bandwidth and slope characteristics.

The estimates of cochlear tuning based on otoacoustic emission (OAE) delays consistently indicate a connection to stimulus level. At lower levels, the delays are longer, although much less than expected based on 1D transmission line models [3, 6, 28]. TEOAE latency gradually reduces with increasing stimulus levels throughout mid-frequency bands, which would suggest a level-dependent decrease in the effective bandwidth of the cochlear filter related to nonlinear cochlear mechanics [28]. When OAE delay data are converted into tuning estimates, both TEOAE- and SFOAE-based measurements exhibit a steady decrease in quality factor as stimulus level increases [3, 6]. This behavior aligns with cochlear models and animal studies suggesting that elevated stimulus levels reduce outer hair cell-mediated gain, resulting in faster traveling wave propagation and broadened basilar membrane responses.

The dependency of tuning on stimulus level varies with frequency; higher frequencies reveal sharper tuning and more pronounced level effects, whereas low frequencies have less sensitivity to level alterations [6]. On the other hand, tuning estimates based on the reflection component of DPOAEs appear to not depend on stimulus level significantly, which may be explained by the fact that the ways they are generated and how sensitive they are to cochlear nonlinearity are quite different [29, 30]. The degree of level dependency varies depending on the analytical approach and delay definition used [3, 5, 28]. These facts must be taken into consideration when comparing tuning estimates coming from different OAE types and stimulus paradigms to behavioral measures of frequency selectivity [7, 23].

Accurate measurements of SFOAE delay may also be useful to identify the characteristic frequency associated with the so-called breakdown of cochlear scaling (or apical–basal transition) which has been observed in several aspects of the cochlear response [13] and OAE phenomenology [29, 31, 32].

An unresolved question is whether the level dependence of SFOAE delay is quantitatively linked to the level dependence of cochlear gain. This question is important because SFOAE delay is often used to estimate cochlear tuning. In simplified linear or resonant cochlear models, a reduction in outer-hair-cell-mediated gain is expected to produce related changes in response bandwidth, wavenumber, and traveling wave delay. Therefore, if gain decreases strongly with increasing stimulus level, delay should also decrease proportionally. However, animal measurements and nonlinear cochlear models suggest that gain may change substantially while delay and tuning change much less. Demonstrating such gain-delay decoupling in human SFOAEs would show that delay-based tuning estimates cannot be interpreted using simple linear gain-scaling assumptions.

The strength of this gain-delay relationship may also vary along the cochlea. Basal cochlear regions approximately obey local scaling symmetry, whereas apical regions show a breakdown of scaling and differ in traveling wave propagation, spatial spread, and phase accumulation. These regional differences could make the level dependence of SFOAE delay stronger below the apical–basal transition than above it. It is therefore important not only to determine whether gain and delay are decoupled overall, but also to test whether the frequency marking the transition between apical and basal response regimes changes with stimulus level. A level-dependent transition would suggest that active cochlear gain helps determine the boundary, whereas a stable transition would favor an explanation based primarily on intrinsic structural and hydrodynamic properties.

Previous studies have described the level dependence of OAE amplitude and latency, and modeling studies have predicted gain-phase decoupling in nonlinear cochlear systems. However, it has not been directly tested in human SFOAEs whether the relative change in delay matches the relative change in gain predicted by linear two-dimensional cochlear models. The present study addresses this gap by isolating the single-reflection SFOAE component using time-frequency

filtering, directly comparing level-dependent changes in gain and delay, and evaluating the measurements against both a linear two-dimensional prediction and a fully nonlinear two-dimensional time-domain model. We additionally use break-point analysis to determine whether the apical–basal transition frequency is stable across stimulus levels.

Methods

Subjects

Twenty young adults with normal hearing ($n = 20$, 13 females) participated in the study. All participants had audiometric thresholds within clinically normal limits (≤ 20 dB HL) across standard frequencies (0.25–8 kHz) in both ears. To ensure consistency across subjects, the ear with the lower threshold at 1 kHz was selected for testing; this was the right ear in 15 participants. All participants reported no history of hearing loss, tinnitus, vestibular or balance problems, or neurological disorders. The study protocol was approved by the University of Texas at Austin Institutional Review Board and written informed consent was obtained from all participants prior to testing.

Stimulus Frequency Otoacoustic Emissions

SFOAEs were recorded using a swept-tone protocol adapted from the approach described by [33]. Signal presentation and data acquisition were managed using a custom software platform (RecordAppX), interfaced with a MOTU 828× audio system (24-bit resolution, 44.1 kHz sampling rate). Sound stimuli were delivered through an ER-10B+ probe microphone assembly fitted with ER-2 insert earphones. The microphone signal was amplified, high-pass filtered at 300 Hz to remove low-frequency noise, and digitized through the MOTU interface. Prior to testing, a depth-compensated calibration procedure was implemented to minimize stimulus delivery variability, particularly between 500 and 5000 Hz [34]. This process involved measuring the half-wave resonance within the ear canal over a 200–20,000 Hz range, estimating insertion depth, and applying an individualized equalization filter to achieve a near-flat frequency response at the tympanic membrane.

A suppressor paradigm was used to measure SFOAEs [35]. Probe levels of 20, 30, and 40 dB SPL were tested in all subjects, with an additional 50-dB SPL probe level included for a subset of four subjects. The order of probe level presentation was randomized across subjects. The suppressor level varied as a function of probe level, following the equation $L_s = 0.6 \times L_p + 42$ and was broadly rounded to the nearest 5-dB step. Both probe and suppressor tones were swept simultaneously from 500 to 4000 Hz at a rate of 0.125 octaves per second. The suppressor frequency was set 10% higher than the probe frequency (frequency ratio = 1.1), and the phase of the suppressor was inverted by 180° on alternating presentations to reduce leakage of the linear suppressor component into the probe-filtered response during averaging. For each condition, 16 probe-alone and 16 probe-plus-suppressor sweeps were collected. A 4-s interval was included between sweeps to mitigate the effects of mechanical adaptation. During data acquisition, real-time monitoring was conducted through RecordAppX to track stimulus fidelity and detect transient artifacts (e.g., motion or swallowing). If transient noise was detected, sweep collection was paused and resumed as necessary to preserve data quality. In addition, offline artifact rejection was performed using a phase-detrending algorithm designed to reduce contamination from residual noise [33]. SFOAEs were derived from the differences between probe-alone and probe-plus-suppressor conditions. A least-squares fit technique was then applied to model the probe and suppressor sweeps and extract the SFOAE response by minimizing the squared error between the measured and predicted signals. Noise floors were computed from pairwise differences of sweeps within each condition, and final estimates of response magnitude, phase, and noise level were calculated separately for analysis.

The derived SFOAE complex spectra were analyzed using a time-frequency (t-f) filtering technique based on the Wavelet transform [36, 37], using two different t-f filtering bands, to select the single-reflection component of the response and to monitor the level of the SFOAE residual in zero-delay region. This way, the estimated group delay is not affected by the presence of SOAEs or by multiple internal reflection components, and the SNR is further improved. After t-f filtering, the signal was averaged over 500-Hz wide frequency bands for statistical analysis, because t-f filtering significantly decreases the frequency resolution. A further double rejection criterion was applied to the filtered data, rejecting (a) the data in the bands with SNR lower than 6 dB and (b) the data showing zero-delay components with level exceeding that of the first reflection component. In these few cases (which we attribute to artifacts because they do not show a reasonable dependence on stimulus level), due to the limited time resolution of the wavelet analysis, the first reflection component delay could have been underestimated. The average delay of the first reflection component was computed as described in Moleti and Sisto [6] as a mean of the delay and weighted for each frequency by the amplitude of the wavelet coefficient. This stable estimate is associated, for each frequency, with the delay of the weighted center of the SFOAE generator distribution, which could be sensitive to the width of the spatial peak of the cochlear response.

Changepoint Analysis to Determine Breaks in Scaling Symmetry

For each subject and probe level, we analyzed the delay–frequency function using a segmented (piecewise linear) regression to characterize changes in delay behavior across frequency. To evaluate the number and significance of breakpoints, we used the segmented R package, which estimates slope change parameters (U-terms) corresponding to each potential breakpoint. For a model with N possible breakpoints, the segmented model estimates U_1, …, U_k, …, U_N, where each U_k quantifies the change in slope at breakpoint k. The presence of a breakpoint is formally tested using a Wald test of H_0: $U_k = 0$ versus H_1: $U_k \neq 0$. Breakpoint k is considered statistically significant if the associated *p*-value is below 0.05.

Model

Contemporary 2D transmission line models and nonlinear cochlear simulations demonstrate that traveling wave delay is shaped by hydrodynamic amplification, viscous dissipation, and level-dependent outer hair cell gain, mechanisms that can alter delay, bandwidth, and gain in a complex way. Thus, a central unresolved problem is whether experimentally measured SFOAE delay truly reflects local cochlear tuning, or whether it is systematically distorted by nonlinear and level-dependent cochlear mechanics. In the WKB approximation, a linearized version of cochlear mechanics is implemented, in which different stimulus levels can be roughly represented by varying a single global parameter related to the effectiveness of the OHC mechanism. Such approximation is sometimes justified by invoking De Boer's NLEQ theorem [38], which is however limited to the response to random noise stimulation. Therefore, one may expect the nonlinear system phase response to deviate more markedly than the amplitude response from that of the "equivalent" linear system. As shown in Sisto et al. [16], comparing simulations of nonlinear models to those of corresponding linear models with the same gain, nonlinear amplifiers change the phase across resulting gain much less than the corresponding linear ones. This behavior, related to the experimentally observed zero-crossing invariance of the impulsive cochlear response [39, 40], suggests that a fully nonlinear model could be necessary for a correct interpretation of the experimental SFOAE phase data.

For each frequency, the group velocity function depends on the derivative with respect to frequency of the real part of the wavenumber:

$$v_g^{-1} = \frac{\partial k}{\partial \omega} \tag{1}$$

,where we omit the real part for brevity.

In that case, in the WKB approximation, the experimental OAE transmission delay would be estimated as a function of frequency as the roundtrip path integral of the reciprocal of the group velocity:

$$\tau(\omega) = -2\int_0^{\hat{x}} dx\prime \frac{\partial k}{\partial \omega}(x\prime, \omega) \tag{2}$$

while the experimental OAE group delay would be obtained as the derivative of the phase accumulated in the roundtrip path:

$$\tau_{\mathrm{OAE}}(\omega) = -2\frac{\partial}{\partial \omega}\int_0^{\hat{x}} dx\prime k(x\prime, \omega) \tag{3}$$

In a scaling cochlea, a partly model-independent relation between OAE roundtrip delay and the peak value of the wavenumber may be obtained [1]:

$$\tau_{\mathrm{OAE}}(\omega) = \frac{2\hat{k}}{k_\omega \omega} \tag{4}$$

Indeed, the spatial and frequency derivatives of the wavenumber are simply related to each other in a scaling symmetric cochlea:

$$\frac{dk}{d\omega} = 0 = \frac{\partial k}{\partial \omega} + \frac{\partial k}{\partial x}\frac{dx}{d\omega} \tag{5}$$

Here we neglect a correction associated with the variation of the phase of the wavenumber [19] that is necessary to fit the chinchilla data but should not be very relevant for humans due to their sharper tuning. More generally, the same correction becomes negligible in a 2D model in the short wave limit, using the 2D wave solution proposed by Duifhuis [20]. Equation (4) implies that, if the peak value of the wavenumber changes with stimulus level, the relative change of the delay would equal that of the peak wavenumber $\hat{k}$:

$$\frac{\Delta\hat{k}}{\hat{k}} = \frac{\Delta\tau_{\mathrm{OAE}}}{\tau_{\mathrm{OAE}}} \tag{6}$$

In a simple 1D (or long wave) representation of the cochlear TW transmission and reflection, neglecting viscosity and 2D hydrodynamics, a rather straightforward relationship between cochlear tuning and the delay of OAEs generated by a single reflection place-fixed mechanism could be expected [9]. Indeed, the following quadratic relation would hold between wavenumber and admittance:

$$k^2 = -2i\omega\rho Y \tag{7}$$

In that approximation, the real part of the wavenumber would cross zero at the CP = BP, where both the admittance and the response would peak. The large nonlinear variation of the gain that is observed experimentally would require a corresponding change of the peak admittance, and of the spatial derivative of the wavenumber. The 1D estimate of the relation between tuning and delay would be approximately quadratic too [9]:

$$\tau_{\mathrm{OAE}}(\omega) \approx \frac{k_0}{\omega k_\omega}\sqrt{Q} \tag{8}$$

A strong anti-damping OHC mechanism, at low stimulus levels, would imply correspondingly peaked admittance, sharp tuning, and long delay.

In the so-called short wave approximation, i.e., where the local wavelength becomes smaller than the cochlear duct height, including 2D hydrodynamics, the relation between admittance and wavenumber is direct proportionality:

$$k = -\frac{2i\omega\rho Y}{H} \tag{9}$$

More important, as shown by experiments [41], the admittance function is not sharply peaked and almost insensitive to stimulus level changes. In other words, the pressure near the BM and the BM velocity have similarly peaked response and similar nonlinear gain range. The weak dependence of the transmission delay on the stimulus level would not be associated with a change of the local group velocity along the path, but with the progressive shift of the response region to basal places with increasing stimulus level. A less effective anti-damping effect from the OHCs would affect indeed the power balance, shifting basally the place where the viscous losses become dominant, causing a sharp drop of the response.

At medium to high levels of stimulus, the basal shift of the response peak is such that the wavenumber is still almost real valued within the whole peak, whereas it would become imaginary at a classical resonant place [18].

In such a modified framework, the main contribution to the peak gain is associated with the focusing effect, i.e., with the local value of the real part of the wavenumber, almost equal to the wavenumber amplitude. The dependence on position of the stiffness-dominated admittance (where the local frequency is much higher than the TW frequency), which is also proportional to the wavenumber in the short wave region, may be schematized as:

$$Y(x) \approx k(x) \approx \omega(x)^{-2}(1 + \mathrm{o}(i\omega/\omega(x)) \approx e^{2k_\omega x} \tag{10}$$

The local response amplitude would grow proportionally to $p(z=0)Y \approx k^2$ and then drop rather abruptly due to viscous damping. Thus, a variation of 3 dB of the response amplitude, conventionally used to define the tuning Q_3, would approximately correspond to:

$$\frac{1}{\sqrt{2}} = \frac{\Delta A_3}{A_{\mathrm{peak}}} = 2\frac{\Delta k_3}{\hat{k}} \approx 4\frac{\Delta\omega(x)_3}{\omega(\hat{x})} \approx \frac{4}{Q_3} \approx 4k_\omega \Delta x_3 \tag{11}$$

This means that in such a simple 2D scaling model, tuning would be independent of frequency and stimulus level:

$$\mathrm{Q}_3 \approx 4\sqrt{2} \tag{12}$$

We remind here that independence of tuning on frequency is one of the expected consequences of cochlear scaling symmetry.

We wish to focus now on the dependence of tuning and OAE delay on the stimulus level. Interestingly, tuning should not even change with level if the response peak is localized in a basal region where the admittance/wavenumber is still dominated by the stiffness component. In 2D models, the position of the response peak is determined by a balance between viscous losses increasing with the wavenumber and OHC anti-damping work. Thus, the region where the imaginary part of the wavenumber is not negligible is reached by the TW only at low stimulus levels, which correspond, for the same wavenumber value, to a stronger OHC active force. At mid to high stimulus levels, a scaling relation between local resonant frequency and wavenumber would hold to a good approximation.

In a 2-D model, both the maximum value of the wavenumber and the peak BM gain decrease with increasing stimulus level in model-dependent ways, but we can estimate them experimentally, measuring the variation of the OAE gain (response divided by the stimulus, both in linear units) with stimulus level, which, for a linear reflection mechanism, should equal that of the BM, and the relative variation of the OAE delay, which should equal that of the peak wavenumber, to check the validity of the short wave WKB prediction:

$$2\Delta\hat{k}(dB) \approx 2\Delta\tau_{\mathrm{OAE}}(dB) = \Delta\hat{G}(dB) \tag{13}$$

In summary, the relation between the bandwidth of the cochlear response and the delay, in a 2D viscous model, would be model dependent and rather difficult to be predicted, while one can check the relation between gain and delay in an almost model-independent way. The main limitation of this theoretical approach is associated with the use of a WKB solution, which neglects important details of the phase behavior [18].

The previous discussion demonstrates how it may be difficult to predict the experimentally observed relation between gain, tuning, and level based on simple and partly model-independent theoretical assumptions. To highlight the decisive role of instantaneous and local nonlinearity, we also

performed numerical simulations using a fully nonlinear cochlear model, including 2D hydrodynamics and the low-pass filtering effect associated with the slow buildup of the OHC transmembrane voltage [16]. The model was solved in the time domain using the Green functions for the pressure and the state space formalism. For more details about this model and its numerical solution, see Moleti and Sisto [42]. SFOAE response was computed by subtracting the response at the cochlear base of a model without roughness from that of the same system with roughness, schematized as a random fluctuation of the local stiffness function of rms amplitude 0.01. In that case, the delay of the response was measured in the time-frequency domain using the wavelet transform and the same definition of average delay used for the analysis of the experimental data.

Results

A typical t-f representation of the SFOAE residual response is shown in Fig. 1 for one subject of this study for three stimulus levels (20, 30, and 40 dB SPL). Within the single-reflection filtering band, isolated spots are visible, corresponding to wave packets of given frequency, bandwidth, and delay.

As noted in previous experimental and modeling studies (e.g., [3, 43]), the localization of the spots is not sensitive to stimulus level, while the relative intensity of the short latency (SL) spots (below the dashed line, within the single reflection band) increases with increasing level. The frequency domain representations of the three filtered responses of the subject of Fig. 1 are shown in Fig. 2 (Left). Even when the filtered single-reflection spectrum coincides almost exactly with the original one, time-frequency filtering improves the SNR of the filtered data [36, 37] as shown in Fig. 2 (Right), where the filtered and unfiltered spectra are compared to the noise floors.

The filtered single-reflection complex spectra may be analyzed in a conventional way, by taking the derivative with respect to frequency of the measured phase function. This way one gets an estimate of the roundtrip transmission delay, which is associated with the cochlear tuning. Unfortunately, this procedure yields a very noisy group delay spectrum, characterized by positive and negative spikes, related to noise and to the residual SFOAE fine structure, associated with the presence of short and long delay components within the first reflection component source. A much smoother and specific measure of cochlear delay of the first reflection component is obtained directly in the t-f domain, by taking, for each frequency, the weighted average of the delay within the corresponding t-f band, using a weight proportional to the local intensity of the wavelet transform [6]. By multiplying the delay by frequency, one gets the alternative representation of Fig. 3, in which the vertical axis represents the dimensionless delay expressed in number of cycles, for the same subject of Figs. 1 and 2. In this representation, one may better appreciate any violation of the scaling symmetry because scaling would imply constant dimensionless delay. In each frequency band, the average latency is represented by a circle of size increasing with increasing stimulus level to show more clearly the slow decrease of delay with increasing stimulus level.

The interpretation of the short latency first reflection components as those associated with more basal sources is confirmed by the analysis of the slope of the I/O functions of the SL and long latency (LL) single-reflection components. As shown in Fig. 4 for the global average over all subjects for all bands, the slope of the SL sources in the low-frequency region is steeper, as expected for sources localized in a more basal region where the gain of the cochlear amplifier is less compressive.

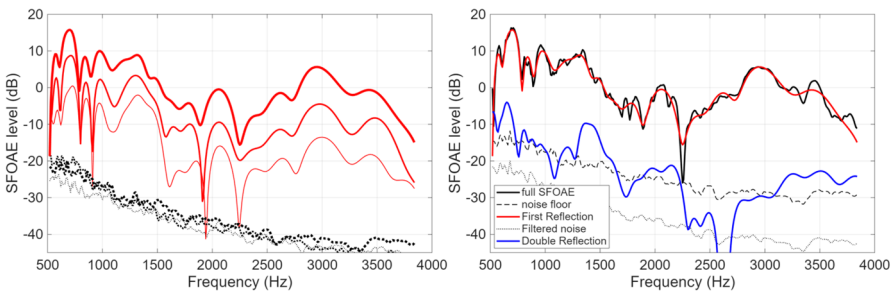

Fig. 2 (Left) Single-reflection filtered component of the SFOAE residual at three different stimulus levels (20, 30, 40 dB SPL). (Right) Although the single-reflection filtered component (thick red line) is almost coincident with the total SFOAE residual (thick black) in this 40 dB case, the advantage of filtering is shown by the reduction of the estimated noise level after filtering (dotted line, with respect to dashed line)

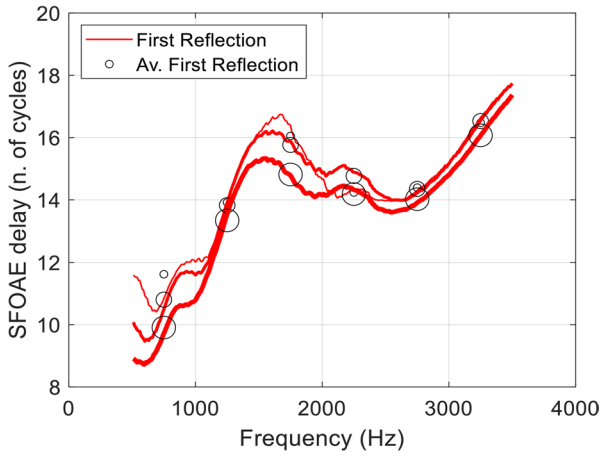

Fig. 3 SFOAE group delay of the subject of Figs. 1 and 2, for three stimulus levels (20, 30, and 40 dB SPL, lines of increasing thickness)

Decoupling Between the Nonlinear Changes of SFOAE Gain and Delay

The asymmetrical nonlinear nature of the response is well represented by plotting (Fig. 5) the gain (left panel), defined as the difference (in dB) between the response and the stimulus level, and the delay (right panel) as a function of frequency, averaged over 500 Hz bands. Tables 1 and 2 provide a summary of paired comparisons of SFOAE gain and delay across probe levels (two-tailed *t*-tests and *p*-values were Benjamini-Hochberg adjusted). Deviation from linear gain is observed, as expected, at all frequencies, while no statistically significant effect of probe level was observed for the delay estimates above 2 kHz.

The decoupling between the nonlinear behavior of gain and phase of the response may be better quantified by plotting the two average quantities $2\Delta\tau_{\mathrm{OAE}}(dB)$ and $\Delta G_{\max}(dB)$ (which, as previously discussed, in a linear 2D model should be almost equal), as a function of frequency, for a stimulus difference of 10 dB (30 and 40 dB SPL). As shown in Fig. 6, the delay change associated with a 10-dB stimulus level change is much smaller than the gain change with respect to the prediction of a linear 2D model. In the same figure, the relative delay and gain changes are also estimated using a fully nonlinear 2D cochlear model solved in the time domain, showing, at least qualitatively, that the strong decoupling observed in the data is also predicted by the nonlinear model.

Breaks in Scaling Symmetry

For each subject and probe level, changepoint analysis was performed on the delay–frequency function using delay expressed in linear time units (ms) as a function of frequency in linear units (Hz). The logarithmic scaling shown in Fig. 7 was used only for visualization and was not used in the segmented regression analysis. Analyses were performed separately for the 6-dB and 12-dB SNR inclusion criteria. For each fitted function, we extracted all slope change parameters, computed the number of estimated breakpoints, and evaluated breakpoint significance using Wald tests on the slope change terms. The Wald tests showed that each curve contained exactly one statistically significant breakpoint, with no evidence for a second breakpoint. Mean breakpoint frequencies were compared across probe levels using paired *t*-tests; however, none of the comparisons reached statistical significance. The breakpoint estimate for the 20-dB SPL probe condition under the 12-dB SNR criterion appeared somewhat displaced relative to the other conditions, likely reflecting greater variability due to the

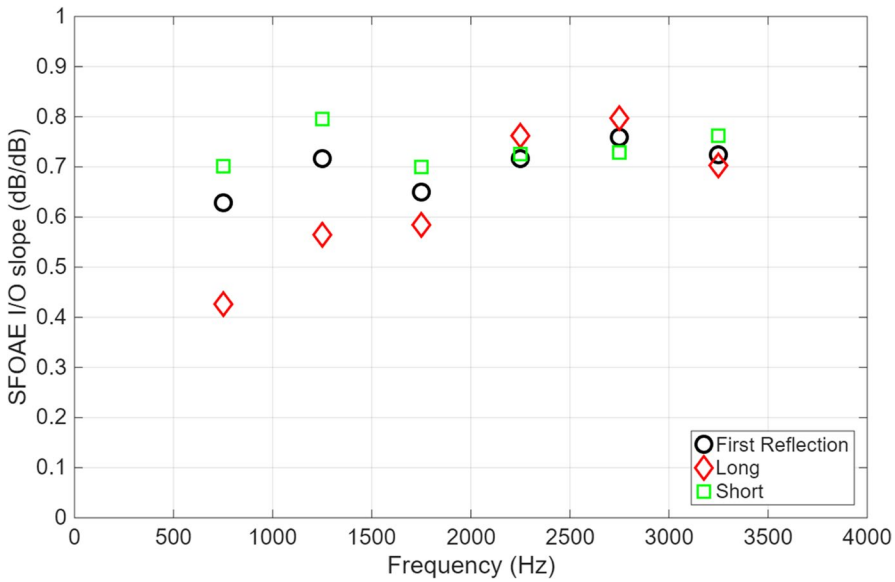

Fig. 4 Steepness of the power law fits to the SFOAE I/O curves for the whole first reflection component (circles), the LL (squares), and the SL (diamonds) first reflection components

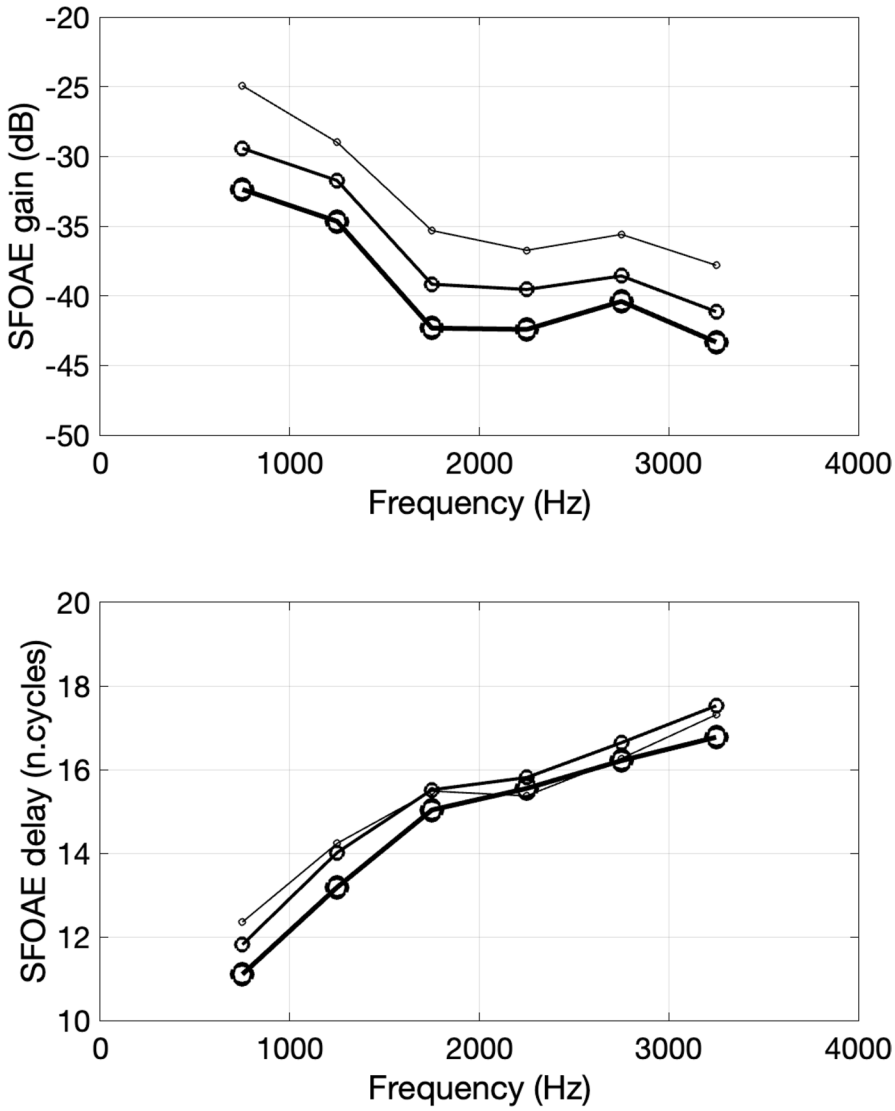

Fig. 5 (Upper panel) Experimental relationship between response gain and stimulus level, and (lower panel) between the delay (in number of cycles) and the stimulus level as a function of frequency, averaged over 500-Hz frequency bands

Table 1 Gain differences (in dB) between SFOAEs to different probe levels (standard deviations are reported in the parenthesis)

Comparisons	750	1250	1750	2250	2750	3250
G(20)-G(30)	4.4 (2.8), df = 13, $p < 0.0001$	2.8 (2.5), df = 16, $p < 0.0001$	3.7 (2.8), df = 10, $p < 0.0001$	2.8 (2.8), df = 8, $p < 0.0001$	3.0 (4.4), df = 7, $p = 0.003$	3.3 (2.4), df = 5, $p = 0.002$
G(30)-G(40)	3.1 (3.8), df = 13, $p < 0.0001$	3.0 (3.0), df = 17, p < 0.0001	2.7 (2.0), df = 14, $p < 0.0001$	2.4 (2.0), df = 14, $p < 0.0001$	2.3 (2.7), df = 10, $p < 0.0001$	1.4 (2.6), df = 9, $p < 0.0001$
G(20)-G(40)	7.4 (4.7), df = 12, $p < 0.0001$	5.7 (3.9), df = 15, $p < 0.0001$	7.0 (3.1), df = 10, $p < 0.0001$	6.0 (3.6), df = 9, p $p < 0.0001$	5.9 (5.1), df = 8, $p < 0.0001$	7.7 (4.8), df = 8, $p < 0.0001$

Table 2 Delay differences (in ms) between SFOAEs to different probe levels (standard deviations are reported in parenthesis)

Comparisons	750	1250	1750	2250	2750	3250
τ(20)-τ(30)	0.6 (0.72), df = 13, $p = 0.004$	0.2 (0.44), df = 18, ns	−0.1 (0.42), df = 17, ns	−0.4 (0.50), df = 12, ns	−0.2 (0.36), df = 11, ns	−0.1 (0.39), df = 8, ns
τ(30)-τ(40)	1.0 (0.99), df = 14, $p = 0.003$	0.7 (0.29), df = 19, $p < 0.0001$	0.3 (0.36), df = 17, $p = 0.01$	0.1 (0.32), df = 15, ns	0.1 (0.23), df = 13, ns	0.1 (0.36), df = 10, $p = 0.03$
τ(20)-τ(40)	1.6 (1.17), df = 13, $p < 0.0001$	0.9 (0.61), df = 18, $p < 0.0001$	0.2 (0.44), df = 17, $p = 0.005$	−0.3 (0.41), df = 14, ns	−0.1 (0.36), df = 10, ns	0.0 (0.28), df = 11, ns

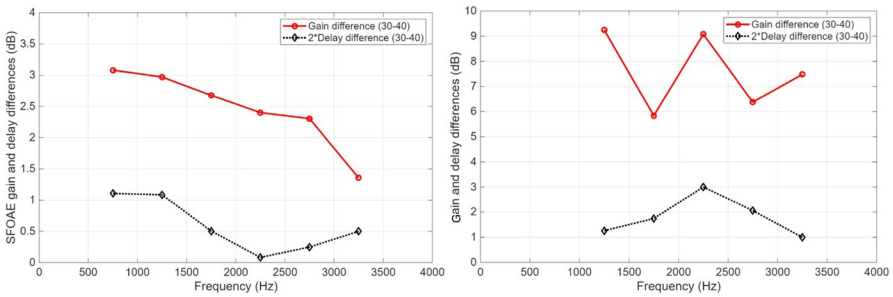

Fig. 6 (Left) Experimental relative variation of SFOAE delay and gain (both in dB units) for a stimulus change of 10 dB (30–40), predicted to be equal in a 2D linear model. (Right) Same comparison from the numerical time-domain solution of a 2D nonlinear cochlear model

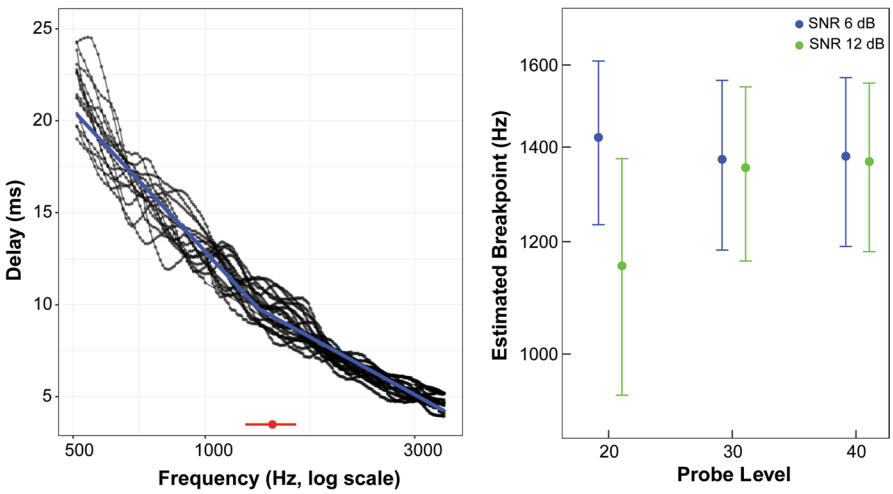

Fig. 7 (Left) Delay–frequency functions for the 20-dB SPL probe level using a 6-dB SNR criterion. Black, individual data; blue, segmented fit; red with error bar, breakpoint estimate with 95% CIs. (Right) Estimated breakpoint frequency at different stimulus levels, showing no significant effect of stimulus level and a characteristic frequency for the breakdown of cochlear scaling of ~ 1.4 kHz

reduced number of retained low-level data points under the stricter SNR criterion. Nevertheless, the overall pattern of a single breakpoint near the apical–basal transition remained consistent across probe levels and SNR criteria.

Discussion

The present results impose a stringent constraint on theoretical descriptions of SFOAE generation: nonlinear compression of SFOAE level does not imply proportional shortening of traveling wave delay. Across frequencies, emission gain decreases robustly with increasing stimulus level, whereas the corresponding phase-gradient delay changes are comparatively small above ~ 1.5 kHz. This systematic gain-delay decoupling is inconsistent with linearized active transmission line models in which changes in OHC effectiveness are represented as a global modification of anti-damping, and confirms previous studies [18].

Within the coherent reflection framework, SFOAEs arise from scattering of the forward traveling wave by distributed micromechanical irregularities. In the linear WKB approximation, the phase-gradient delay of the single-reflection component is governed by the accumulated phase of the forward and backward slow waves and is therefore directly related to the local wavenumber distribution along the cochlear partition [4]. Under simplified active models, a reduction in OHC gain broadens the spatial envelope of the response, shifts the peak basally, and reduces the effective roundtrip propagation distance. Such models predict that amplitude compression with increasing stimulus level should be accompanied by a commensurate reduction in phase-gradient delay. The experimental data do not exhibit this proportionality. Although gain decreases by several decibels per 10-dB increase in probe level, delay changes are substantially smaller than predicted by linear models adjusted to match the observed amplitude compression. This discrepancy indicates that nonlinear cochlear amplification cannot be adequately described as a uniform scaling of active feedback. Instead, the data imply that nonlinear amplification redistributes energy spatially without producing large shifts in the cumulative phase accumulation along the traveling wave path.

While the nonlinear gain was quite evident and statistically significant, the effect of level on delay was relatively less pronounced above 1.5 kHz. This finding is broadly consistent with previous time-domain studies of OAE latency. Rasetshwane et al. [44] reported orderly reductions in tone-burst OAE latency with increasing

stimulus level across a broad frequency range, although the magnitude of latency shortening remained comparatively modest relative to nonlinear amplitude changes. Abdala et al. [45] reported a steady slow decrease of SFOAE delays with increasing stimulus level over a wide level and frequency range. Similarly, Dalhoff et al. [46] reported pulse DPOAE latency reductions of approximately 35% across stimulus levels from 25 to 85 dB SPL, with no strong systematic frequency dependence above approximately 1–2 kHz, corresponding to 1.2 dB (15%) change in our 20 dB level range, similar to the results of the present study. Importantly, those pulse DPOAE measurements were obtained directly in the time domain from the nonlinear-distortion component. Although methodological differences across SFOAE, tone-burst OAE, and pulse DPOAE paradigms complicate direct quantitative comparisons, these approaches converge in suggesting that OAE delay exhibits measurable but comparatively modest dependence on stimulus level relative to the substantially larger nonlinear changes observed in cochlear gain.

Importantly, the absolute delay magnitudes and their frequency dependence remain consistent with transmission line interpretations and with WKB descriptions of slow-wave backward propagation [4, 21, 22]. Thus, the fundamental linear relation between delay and wavenumber remains intact. The breakdown occurs specifically in the nonlinear regime: level-dependent reductions in gain do not translate into proportional modifications of the effective propagation time. Recent linear nonresonant formulations of the cochlear response peak predict delay variations several times larger than those observed here when active gain is reduced [18]. The experimental findings therefore indicate that nonlinear spatial-mechanical interactions constrain phase accumulation more strongly than predicted by linearized gain-scaling models.

The qualitative agreement between the measurements and the fully nonlinear two-dimensional time-domain model supports this interpretation. In the nonlinear model, OHC gain modifies the balance between pressure focusing and viscous losses in a spatially dependent manner. As stimulus level increases, the effective anti-damping decreases, but the resulting changes in wavenumber growth and peak location are partially compensated by hydrodynamic focusing and distributed damping. Consequently, substantial compression of emission amplitude can occur with relatively small shifts in the integrated phase of the traveling wave [18]. The data therefore favor a nonlinear spatial redistribution mechanism over global gain-scaling representations of cochlear nonlinearity. The frequency dependence of the delay changes further constrains theory. Significant level effects are confined primarily to frequencies below ~ 1.5 kHz, i.e., in the region associated with the breakdown of cochlear scaling. Apical traveling waves extend over broader spatial regions and exhibit slower wavenumber growth, rendering their phase accumulation more sensitive to modest shifts in peak location. In basal regions, where pressure focusing and viscous losses increase more steeply with wavenumber, the spatial response is more tightly confined, and the cumulative phase is less susceptible to level-dependent migration of the response maximum. This spatial asymmetry suggests that propagation delay is governed predominantly by geometric and hydrodynamic constraints rather than by instantaneous amplifier gain.

The breakpoint analysis reveals a single scaling symmetry transition near 1.4 kHz that is invariant across stimulus levels [29, 31, 32]. The reduced level dependence of delay observed above this breakpoint is consistent with the approximate local scaling symmetry that characterizes basal cochlear mechanics, where traveling wave propagation and phase accumulation vary more systematically with frequency and are less sensitive to level-dependent shifts in the response peak [5, 47]. In contrast, apical regions exhibit weaker scaling behavior, broader spatial excitation patterns, and more gradual phase accumulation, rendering propagation delay more sensitive to changes in stimulus level and response peak location [13, 47, 48]. These findings therefore suggest that the apical–basal transition is strongly influenced by intrinsic structural and hydrodynamic properties of the cochlea rather than arising solely from nonlinear modulation of active feedback. Thus, the symmetry break appears to mark a geometric transition in cochlear mechanics rather than a purely dynamical consequence of OHC activation.

The present findings do not invalidate the use of SFOAE delay as an indicator of cochlear tuning. Rather, they limit the conditions under which delay can be converted directly into a quantitative tuning estimate. Delay remains related to traveling wave phase accumulation and local wavenumber and therefore retains information about cochlear mechanics. However, the observed gain-delay decoupling shows that changes in delay cannot be assumed to track changes in cochlear gain, response bandwidth, or tuning in a fixed proportion across stimulus levels. Thus, delay-based tuning estimates derived from simple resonant or globally linearized models may need to be cautiously applied to the nonlinear cochlea.

A fully nonlinear model could, in principle, provide improved tuning estimates by jointly predicting basilar membrane bandwidth, SFOAE gain, and SFOAE delay for the same stimulus conditions. Such a model would allow a measured delay to be interpreted within a level- and frequency-dependent mechanical framework rather than through a fixed analytical conversion. In the present study, however, the nonlinear model was used only to test whether it could reproduce the qualitative decoupling between gain and delay. We did not independently validate its predicted tuning or derive an inverse mapping from SFOAE delay to tuning. Therefore, the current results should be regarded as

constraints on future delay-to-tuning models rather than as a new quantitative method for estimating tuning.

Taken together, these findings refine the theoretical interpretation of SFOAE delay as an index of cochlear tuning. Classical delay–bandwidth relations assume proportionality between roundtrip delay and filter sharpness. The present results demonstrate that, under nonlinear cochlear mechanics, delay does not scale proportionally with gain compression. Consequently, delay-based tuning estimates must be interpreted within nonlinear transmission line frameworks that incorporate spatial redistribution of amplification and viscous losses.

Conclusions

This study confirms the strong decoupling between nonlinear gain and delay changes in the cochlea, to an extent that is theoretically predicted only by fully nonlinear models [18]. The group delay of SFOAEs is weakly sensitive to stimulus level changes in the 20–40-dB stimulus level range, while the gain changes significantly in the same range. Model-independent predictions using general properties of 2D transmission line linear models would predict a much stronger relationship between the two variations, while a 2D nonlinear model solved in the time domain agrees qualitatively with the data, predicting delay changes much smaller than the corresponding gain changes.

Author Contribution Conceptualization: AM, RS, and SKM. Data collection: SKM. Data analysis: AM, HR, TB, YS, and RS. Visualization: AM, TB, HR, and YS. Supervision: AM and SKM. Writing, reviewing, and editing: AM, YS, and SKM.

Funding HR and SKM: work was partly supported by an NIH/NIDCD grant R01DC018046.

Data Availability The data and codes used will be made available on reasonable request.

Declarations

Ethics Approval The study protocol was approved by the University of Texas at Austin Institutional Review Board and written informed consent was obtained from all participants prior to testing.

Competing Interests The authors declare no competing interests.

Use of AI No AI in writing/grammar and figures/artwork was used.

References

1. Talmadge CL, Tubis A, Long GR et al (1998) Modeling otoacoustic emission and hearing threshold fine structures. J Acoust Soc Am 104:1517–1543. https://doi.org/10.1121/1.424364
2. Shera CA, Tubis A, Talmadge CL (2005) Coherent reflection in a two-dimensional cochlea: short-wave versus long-wave scattering in the generation of reflection-source otoacoustic emissions. J Acoust Soc Am 118:287–313. https://doi.org/10.1121/1.1895025
3. Sisto R, Sanjust F, Moleti A (2013) Input/output functions of different-latency components of transient-evoked and stimulus-frequency otoacoustic emissions. J Acoust Soc Am 133(4):2240–2253. https://doi.org/10.1121/1.4794382
4. Sisto R, Moleti A, Shera CA (2015) On the spatial distribution of the reflection sources of different latency components of otoacoustic emissions. J Acoust Soc Am 137(2):768–776. https://doi.org/10.1121/1.4906583
5. Shera CA, Guinan JJ Jr, Oxenham AJ (2002) Revised estimates of human cochlear tuning from otoacoustic and behavioral measurements. Proc Natl Acad Sci 99(5):3318–3323. https://doi.org/10.1073/pnas.032675099
6. Moleti A, Sisto R (2016) Estimating cochlear tuning dependence on stimulus level and frequency from the delay of otoacoustic emissions. J Acoust Soc Am 140:945–59. https://doi.org/10.1121/1.4960588
7. Oxenham AJ, Shera CA (2003) Estimates of human cochlear tuning at low levels using forward and simultaneous masking. J Assoc Res Otolaryngol 4(4):541–554. https://doi.org/10.1007/s10162-002-3058-y
8. Aryal S, Mishra S (2026) On the sharpness of auditory filters: considering subclinical deficits reveals sharper otoacoustic emission estimates of frequency selectivity in humans. J Assoc Res Otolaryngol. https://doi.org/10.1007/s10162-025-01018-8
9. Moleti A, Sisto R (2003) Objective estimates of cochlear tuning by otoacoustic emission analysis. J Acoust Soc Am 113:423–429. https://doi.org/10.1121/1.1523389
10. Moleti A, Sisto R, Tognola G et al (2005) Otoacoustic emission latency, cochlear tuning, and hearing functionality in neonates. J Acoust Soc Am 118:1576–84. https://doi.org/10.1121/1.2000769
11. Moleti A, Sisto R, Paglialonga A et al (2008) Transient evoked otoacoustic emission latency and estimates of cochlear tuning in preterm neonates. J Acoust Soc Am 124:2984–94. https://doi.org/10.1121/1.2977737
12. Charaziak K, Shera C (2021) Reflection-source emissions evoked with clicks and frequency sweeps: comparisons across levels. J Assoc Res Otolaryngol. https://doi.org/10.1007/s10162-021-00813-3
13. Robles L, Ruggero M (2001) Mechanics of the mammalian cochlea. Physiol Rev. https://doi.org/10.1152/physrev.2001.81.3.1305
14. Cooper NP, Vavakou A, van der Heijden M (2018) Vibration hotspots reveal longitudinal funneling of sound-evoked motion in the mammalian cochlea. Nat Commun 9:3054. https://doi.org/10.1038/s41467-018-05483-z

15. Cho NH, Puria S (2022) Cochlear motion across the reticular lamina implies that it is not a stiff plate. Sci Rep 12:18715. https://doi.org/10.1038/s41598-022-23525-x
16. Sisto R, Moleti A, Altoè A (2015) Decoupling the level dependence of the basilar membrane gain and phase in nonlinear cochlea models. J Acoust Soc Am. https://doi.org/10.1121/1.4928291
17. Sisto R, Moleti A (2021) Low-passed outer hair cell response and apical-basal transition in a nonlinear transmission-line cochlear model. J Acoust Soc Am 149:1296–305. https://doi.org/10.1121/10.0003569
18. Sisto R, Moleti A (2024) The tonotopic cochlea puzzle: a resonant transmission line with a "non-resonant" response peak. JASA Express Lett. https://doi.org/10.1121/10.0028020
19. Shera CA, Tubis A, Talmadge CL (2008) Testing coherent reflection in chinchilla: auditory-nerve responses predict stimulus-frequency emissions. J Acoust Soc Am 124:381–395. https://doi.org/10.1121/1.2917805
20. Duifhuis H (2011). Modeling the nonlinear cochlea. In: Cochlear mechanics. Springer, Boston, MA. https://doi.org/10.1007/978-1-4419-6117-4_5
21. Moleti A, Sisto R (2008) Comparison between otoacoustic and auditory brainstem response latencies supports slow backward propagation of otoacoustic emissions. J Acoust Soc Am 123(3):1495–1503. https://doi.org/10.1121/1.2836781
22. Harte JM, Pigasse G, Dau T (2009) Comparison of cochlear delay estimates using otoacoustic emissions and auditory brainstem responses. J Acoust Soc Am 126:1291–1301. https://doi.org/10.1121/1.3168508
23. Glasberg BR, Moore BCJ (1990) Derivation of auditory filter shapes from notched-noise data. Hear Res 47:103–138. https://doi.org/10.1016/0378-5955(90)90170-T
24. Weber D (1986) Procedure-independent growth-of-masking functions. J Acoust Soc Am. https://doi.org/10.1121/1.393168
25. Ewert S, Dau T (2000) Characterizing frequency selectivity for envelope fluctuations. J Acoust Soc Am. https://doi.org/10.1121/1.1288665
26. Nelson D, Chargo S, Kopun J et al (1990) Effects of stimulus level on forward-masked psychophysical tuning curves in quiet and in noise. J Acoust Soc Am. https://doi.org/10.1121/1.400111
27. Lopez-Poveda E, Aguilar E, Johannesen P et al (2013) Contralateral efferent regulation of human cochlear tuning: behavioural observations and computer model simulations. Adv Exp Med Biol. https://doi.org/10.1007/978-1-4614-1590-9_6
28. Sisto R, Moleti A (2007) Transient evoked otoacoustic emission latency and cochlear tuning at different stimulus levels. J Acoust Soc Am 122:2183–2190. https://doi.org/10.1121/1.2769981
29. Dhar S, Rogers A, Abdala C (2011) Breaking away: violation of distortion emission phase-frequency invariance at low frequencies. J Acoust Soc Am 129:3115–3122. https://doi.org/10.1121/1.3569732
30. Whitehead ML, Stagner BB, Martin GK et al (1996) Visualization of the onset of distortion-product otoacoustic emissions, and measurement of their latency. J Acoust Soc Am 100:1663–1679. https://doi.org/10.1121/1.416065
31. Moleti A, Pistilli D, Sisto R (2017) Evidence for apical-basal transition in the delay of the reflection components of otoacoustic emissions. J Acoust Soc Am 141:116–126. https://doi.org/10.1121/1.4973866
32. Abdala C, Dhar S, Mishra S (2011) The breaking of cochlear scaling symmetry in human newborns and adults. J Acoust Soc Am 129:3104–3114. https://doi.org/10.1121/1.3569737
33. Mishra SK, Talmadge CL (2018) Sweep-tone evoked stimulus frequency otoacoustic emissions in humans: development of a noise-rejection algorithm and normative features. Hear Res 358:42–49. https://doi.org/10.1016/j.heares.2017.11.006
34. Lee J, Dhar S, Abel R et al (2012) Behavioral hearing thresholds between 0.125 and 20 kHz using depth-compensated ear simulator calibration. Ear Hear 33:315–329. https://doi.org/10.1097/AUD.0b013e31823d7917
35. Kemp DT, Chum RA (1980) Observations on the generator mechanism of stimulus frequency acoustic emissions — two tone suppression. In: Van Den Brink G, Bilsen FA (eds) Psychophysical, physiological and behavioural studies in hearing. Dordrecht: Springer Netherlands, pp 34–42. https://doi.org/10.1007/978-94-009-9144-6_5
36. Moleti A, Longo F, Sisto R (2012) Time-frequency domain filtering of evoked otoacoustic emissions. J Acoust Soc Am 132:2455–2467. https://doi.org/10.1121/1.4751537
37. Moleti A (2024) Optimal scale-invariant wavelet representation and filtering of human otoacoustic emissions. J Assoc Res Otolaryngol. https://doi.org/10.1007/s10162-024-00943-4
38. de Boer E (1997) Connecting frequency selectivity and nonlinearity for models of the cochlea. Aud Neurosci 3:377–388
39. Shera CA (2001) Intensity-invariance of fine time structure in basilar-membrane click responses: implications for cochlear mechanics. J Acoust Soc Am 110:332–348. https://doi.org/10.1121/1.1378349
40. Sisto R, Shera CA, Altoè A, Moleti A (2019) Constraints imposed by zero-crossing invariance on cochlear models with two mechanical degrees of freedom. J Acoust Soc Am 146(3):1685–1695. https://doi.org/10.1121/1.5126514
41. Dong W, Olson ES (2013) Detection of cochlear amplification and its activation. Biophysical Journal 105(4):1067–1078. https://doi.org/10.1016/j.bpj.2013.06.049
42. Moleti A, Sisto R (2025) Mathematical Models of the Cochlear Function. In: Optimizing the diagnostic power of otoacoustic emissions using theoretical cochlear mechanics. Springer-AAS Acoustics Series. Springer, Cham. https://doi.org/10.1007/978-3-031-90514-8_3
43. Moleti A, Mohsin Al-Maamury A, Bertaccini D et al (2013) Generation place of the long- and short-latency components of transient-evoked otoacoustic emissions in a nonlinear cochlear model. J Acoust Soc Am 133:4098–108. https://doi.org/10.1121/1.4802940
44. Rasetshwane DM, Argenyi M, Neely ST et al (2013) Latency of tone-burst-evoked auditory brain stem responses and otoacoustic emissions: level, frequency, and rise-time effects. J Acoust Soc Am 133:2803–2817. https://doi.org/10.1121/1.4798666
45. Abdala C, Luo P, Shera CA (2022) Characterizing the relationship between reflection and distortion otoacoustic emissions in normal-hearing adults. J Assoc Res Otolaryngol 23:647–664
46. Dalhoff E, Zelle D, Bader K (2025) Latencies of pulsed distortion-product otoacoustic emissions and their relation to auditory brainstem responses. J Assoc Res Otolaryngol 27:83–105. https://doi.org/10.1007/s10162-025-01019-7
47. Cooper NP, Manley GA, Shera CA, et al (2011) Comparative auditory mechanics: from species to species and from base to apex—a moderated discussion, Williamstown, Massachusetts (USA), pp 701–6. https://doi.org/10.1063/1.3658172
48. Recio-Spinoso A, Oghalai JS (2017) Mechanical tuning and amplification within the apex of the guinea pig cochlea. J Physiol 595:4549–4561. https://doi.org/10.1113/JP273881